Bresler, J.; Neumeier, S.; Ziener, M.; Pyczak, F.; Göken, M.:
The influence of niobium, tantalum and zirconium on the microstructure and creep strength of fully lamellar γ/α2 titanium aluminides.
In: Materials Science and Engineering A. Vol. 744 (2019) 46 - 53.
First published online by Elsevier: 01.12.2018

https://dx.doi.org/10.1016/j.msea.2018.11.152

The influence of Niobium, Tantalum and Zirconium on the microstructure and creep strength of fully lamellar γ/α_2 Titanium Aluminides

J. Bresler[a], S. Neumeier[a], M. Ziener[a], F. Pyczak[b], M. Göken[a]

[a] Friedrich-Alexander-Universität Erlangen-Nürnberg (FAU), Materials Science & Engineering, Institute I, Martensstr. 5, 91058 Erlangen, Germany

[b] Institute of Materials Research, Helmholtz-Zentrum Geesthacht, Max-Planck-Str. 1, 21502 Geesthacht, Germany

---

Abstract

Titanium aluminides are excellent materials for light-weight applications at high temperatures. To enhance their creep strength, various alloying elements are added. In this work the effect of 5 at% Niobium (Nb), Tantalum (Ta) and Zirconium (Zr) on the creep properties of ternary Ti-44Al-5X (X=Nb, Ta, Zr) with a fully lamellar microstructure, is systematically studied. These alloying elements have a high solubility in titanium aluminides, and show a different α_2/γ partitioning behavior as well as a different influence on the lattice parameters of both phases. The average interface distance between the α_2- and γ-phase is adjusted to about 300 nm by the cooling rate to evaluate the influence of the three alloying elements. The creep tests reveal that all three alloying elements increase the creep resistance of titanium aluminides, particularly Ta and Zr. Ta seems to extend the pronounced primary creep regime, whereas Zr seems to reduce it. The alloying elements decrease also the lamellar spacing compared to the binary alloy. Microstructural investigations after the creep tests show a beneficial effect of the alloying elements on the microstructural stability during creep exposure, since they retard the discontinuous coarsening rate.

Keywords: Titanium aluminides; microstructure; alloying elements; creep;

---

1. Introduction

Titanium aluminides are one of the most promising materials in industrial applications where a low density and high strength at elevated temperatures are needed. With a density of 3.8 - 4.3 g/cm^3 they possess a high specific strength which makes them attractive for rotating loaded components [1]. They are good alternative materials to replace the commonly used nickel-based superalloys in some applications like turbochargers or turbine blades in the low pressure section of aircraft engines [2,3]. For such applications, the creep properties of these intermetallic alloys are of particular importance.

The creep resistance is significantly governed by the microstructure, which can be tailored by the heat treatment. Investigations have shown that a fully lamellar microstructure exhibits the best creep resistance in comparison to other microstructures like near-gamma, duplex or nearly-lamellar microstructure [4]. A fully lamellar microstructure consists of alternating lamellae of the two intermetallic phases α_2 and γ. The α_2-phase has a hexagonal unit cell with $D0_{19}$-structure and the chemical composition Ti_3Al, while the TiAl γ-phase has a tetragonal distorted face centered cubic like unit cell with $L1_0$-structure. The crystallographic relationship between these two alternating phases is described by the Blackburn orientation relationship [5]:

$$(0001)_{\alpha_2} \parallel \{111\}_{\gamma} \text{ and } \langle 11\bar{2}0\rangle_{\alpha_2} \parallel \langle 1\bar{1}0]_{\gamma}$$

The slight difference in the lattice parameters of both phases lead to a semi-coherent interface. The different lattice spacing at the interface is described through the misfit and varies with the chemical composition of the alloy, thermal expansion coefficient and temperature [6]. The lattice misfit induces coherency stresses and therefore interfacial dislocations can frequently be found at the interface [7–9].

To enhance the creep properties of fully lamellar titanium aluminides other alloying elements can be added [10]. Studies on minor alloying elements that form precipitates, like boron and carbon, or alloying elements that have a higher solubility in γ and α_2, such as Cr, Nb, Si, Ta, V and Zr, demonstrated that alloying elements can improve the creep resistance [10–15]. Kainuma et al. [16] made a systematic experimental study on the phase equilibria of twelve common alloying elements and their partitioning behavior between the present phases. This investigation pointed out, that there are only a few elements like Nb, Ta and Zr, that have a solubility of more than 5 at.% in the two-phase field (α_2/γ). Therefore, these elements are considered as suitable strengthening elements for titanium aluminides. Nb is a common alloying element in titanium aluminides and its influence on creep properties, oxidation and deformation mechanisms has been well studied [17–19]. Ta is also used as an alloying element in titanium aluminides, but not as frequently as Nb. A few papers investigated its influence on the microstructure compared to a Nb-containing alloy and the formation of precipitates [20,21]. In the case of the alloying element Zr, Cheng et al. assumed that Zr increases the creep properties, but the investigated alloy in their work are four different alloying elements and thus no effect could be attributed directly to Zr [22]. It was also reported that the addition of Zr increases the yield stress at intermediate temperatures, as well as the fracture strain [23]. In a further study, all three elements Nb, Ta and Zr, were alloyed with up to 8 at.% [24]. Through the high alloying content and the presence of the minor elements silicon and boron a microstructure consisting of α_2-, β- and γ-phase resulted. A clear separation between the influences of each alloying element therefore was not possible.

A noticeable difference of the three alloying elements is their partitioning between the phases. Nb partitions nearly in equal parts to the two phases, whereas Ta partitions predominantly to the α_2-phase and Zr mainly to the γ-phase, according to Kainuma et al. [16].

In this study the influence of the three elements Nb, Ta and Zr on the creep properties in a fully lamellar microstructure was investigated. Several studies have shown that these elements have the potential to increase the creep properties [13,16,24–26], but no systematic investigation on their influence on creep strength, the underlying mechanisms and how their effects differ compared to a binary alloy exists so far. To separate the influence of the alloying elements from other effects, the alloying element content, the α_2/γ-interface spacing and applied stresses in the creep tests were kept constant.

2. Experimental methods

The investigated binary Ti-44Al alloy as well as the ternary Ti-44Al-5X (X=Nb, Ta, Zr) alloys were manufactured via vacuum arc melting from technically pure metals at the Helmoltz-Zentrum in Geesthacht, the nominal and measured composition is displayed in Table 1. The melted buttons had a diameter of around 30 mm and a height of 15 mm. The nominal compositions are given in atomic percentage. The as-cast alloys were solution heat treated for 1 h at 1380°C in argon atmosphere. Afterwards samples of all four alloys were cooled at different cooling rates, between 0.5 K/min and 10 K/min to study the effect of the alloying elements on the width of the lamellae.

Table 1

Nominal and measured composition (EDX in brackets) in at.% of the investigated Ti-44Al and Ti-44Al-5X (X= Nb, Ta, Zr) alloys

	Ti	Al	Nb	Ta	Zr
Ti-44Al	56 (57.18)	44 (42.82)	-	-	-
Ti-44Al-5Nb	51 (52.35)	44 (42.19)	5 (5.46)	-	-
Ti-44Al-5Ta	51 (52.99)	44 (41.92)	-	5 (5.09)	-
Ti-44Al-5Zr	51 (51.59)	44 (42.92)	-	-	5 (5.49)

The density of the investigated alloys was determined via Archimedes principle, using a Mettler Toledo AG204 scales. The measured specimens were 4 mm in diameter and 16 mm in height.

The creep experiments were performed under compression in air at a temperature of 900°C. Cylindrical specimens were wire eroded to 4.2 mm in diameter out of the buttons, heat treated, turned to 4 mm diameter and ground plan-parallel to a height of 6 mm. Each alloy was tested at constant stress of 100 MPa, 150 MPa, 200 MPa and 250 MPa to a plastic strain of around 5 %.

The microstructure analysis and the energy dispersive X-ray spectroscopy (EDX) were performed in a ZEISS Cross Beam 1540 ESB focused ion beam scanning electron microscope (SEM) using a back-scattered electron detector (BSD) from K. E. Developments Ltd. and IncaPenta5X (EDX) from Oxford Instruments. EDX measurements were performed using 8 mm working distance and 20 kV excitation voltage. The specimens were ground and then electropolished at 50 V and -30°C for 5 - 10 s (electrolyte A2-I, Struers GmbH, Germany).

The local chemical composition was determined by an electron probe microanalysis (EPMA) system using a JEOL JXA-8100. 160 µm^2 large areas were investigated with a spot size of 500 nm, a step size of 2.5 µm and a dwell time of 150 ms.

To evaluate the primary creep regime, the Garofalo-equation (equation 1) [27] was used to fit the experimentally measured strain (ε) – time (t) curves, in a simple empirical approach.

$$\varepsilon = \varepsilon_0 + \varepsilon_I[1 - exp(-rt)] + \dot{\varepsilon}_{II} \cdot t \quad (1)$$

The first term ε_0 describes the initial strain at the beginning of the experiment and is related to the elastic deformation after applying the load. The parameter ε_I is the strain in the transient

region and specifies the strain at which the equilibrium of dislocation emission and thermally activated dislocation annihilation is achieved. The parameter r is the transition period and determines the length of the primary creep regime. To determine r and ε_I, a least-square fit method is used. The third term of the equation is the constant strain rate in the secondary creep regime, $\dot{\varepsilon}_{II}$, multiplied with the time, t. In Figure 1 the first part of the creep curve of the Ti-44Al-5Nb alloy loaded with 100 MPa is displayed, as an example.

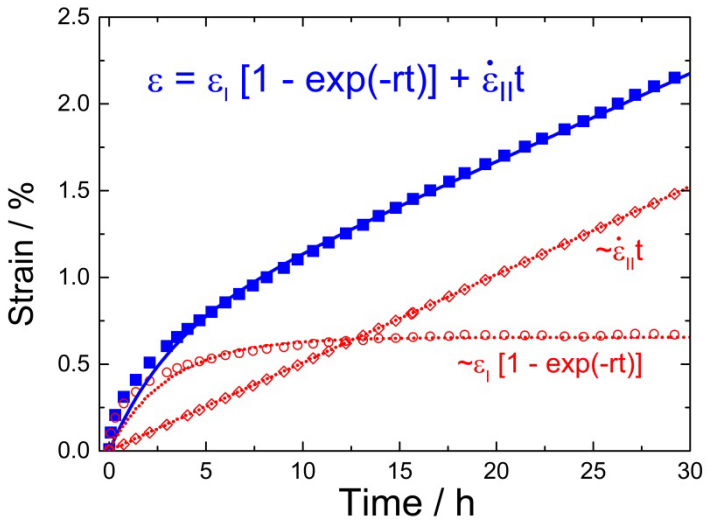

Figure 1 Creep curve (strain vs. time) of Ti-44Al-5Nb at 900°C (filled squares) with the Garofalo-fit (blue line) in the range of 2.5 % plastic deformation. The fitted total curve is the sum of the two terms of equation 1 (open symbols, red dashed lines).

3. Results

In the following, the influence of the three alloying elements on α_2/γ-interface spacing, density, cast microstructure, creep properties and microstructural stability during the creep exposure is presented.

3.1 Average spacing between α_2/γ-interfaces

Titanium aluminides with a fully lamellar microstructure show the best creep strength in comparison with other possible microstructures. These superior creep properties are mainly

related to the α_2/γ-interface, which represents the most effective barrier for dislocation movement. Several studies have shown, that γ/γ-interfaces and domain boundaries also retard the dislocation movement and retard the plastic deformation, but not in such a pronounced way like the α_2/γ-interface [28,29]. Due to the fact that the α_2-phase and the γ-phase have no common slip system, the dislocation movement is immobilized at the interface between these two phases in comparison to the γ/γ-interface [28,29]. This means the main influence on the creep properties is related to the average distances between the α_2/γ-interfaces and not the colony size and the colony boundaries [30–32]. In order to test the influence of the alloying elements on the creep properties, all alloys have to have a microstructure with equal average α_2/γ-interface spacing. The average width of the lamellae is adjusted by the cooling rate after the solution heat treatment in the single α-phase field. The formation of the lamellae is an eutectoid transformation reaction and generates the fully lamellar microstructure [8,33]. Figure 2a displays the relationship between average α_2/γ-interface spacing and cooling rate for the four investigated alloys.

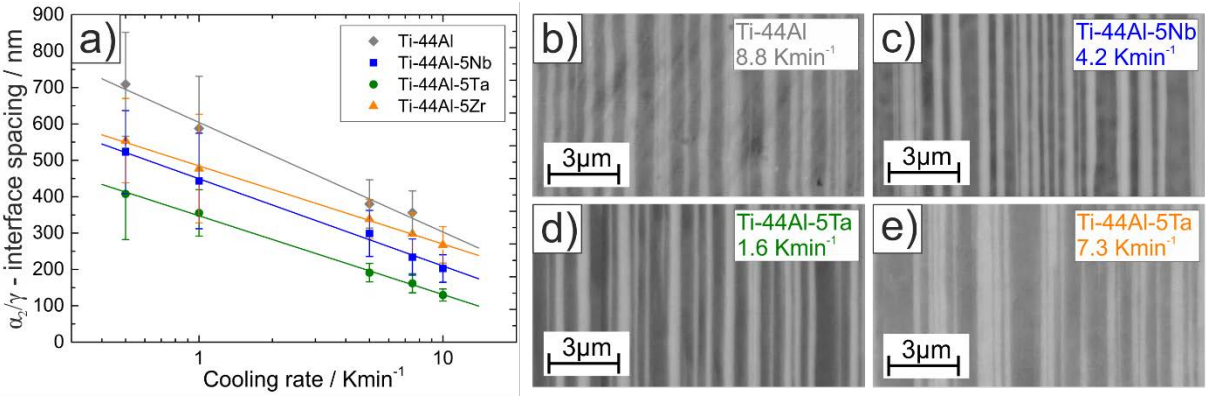

Figure 2 a) Average α_2/γ-interface spacing of the four investigated alloys as a function of the cooling rate after heating at 1380°C for 1 h. (b-e) Adjusted microstructure with similar average α_2/γ-interface spacing of around 300 nm for subsequent creep tests with corresponding cooling rates.

It is clear, that the alloying elements and cooling rates have a significant influence on the width of the lamellae, and thus on the average distance of the α_2/γ-interfaces. In the range of

0.5 K/min up to 10 K/min Ti-44Al exhibits the largest average spacing, followed by Ti-44Al-5Zr and Ti-44Al-5Nb. Ti-44Al-5Ta has the smallest one in the investigated range of cooling rates. As known from literature [34,35], the γ lamellae can nucleate through several processes, i.e. a heterogeneous transformation occurring at grain boundaries, a homogeneous transformation in the α_2 matrix and an interfacial transformation. The lamellar spacing is affected by the rate of nucleation and thickening of the lamellae. The nucleation rate depends amongst others on the driving force and thus on undercooling, the interfacial energy of the generated interfaces, and the activation energy of atomic mobility [36]. The thickening of lamellae depends on the diffusion of elements. In comparison to the binary Ti-44Al, the smaller α_2/γ-interface spacing in Ti-44Al-5Zr could be caused by the shift of the α-transus temperature to higher temperatures [37] and thus a stronger undercooling and higher driving force for nucleation. In contrast, Nb and Ta shift the α-transus temperature to lower temperatures, but Nb is known to have a significantly lower interdiffusion coefficient in comparison to Zr [34], which would lead to a slower thickening rate of the lamellae. Assuming that the diffusivity of Ta is even lower than that of Nb, the differences in the α_2/γ-interface spacings between Ti-44Al-5Nb and Ti-44Al-5Ta could be also explained. However, further studies on the influencing parameters, such as the interdiffusion coefficients, interfacial energies as well as the partitioning behavior of the alloying elements between the different phases are needed to fully explain the observed results.

Based on these experiments, a cooling rate of 8.8 K/min for Ti-44Al, 4.2 K/min for Ti-44Al-5Nb, 1.6 K/min for Ti-44Al-5Ta and 7.3 K/min for Ti-44Al-5Zr was chosen for the creep specimens to achieve a similar microstructure with an average α_2/γ-interface spacing of around 300 nm. Measurements of the lamellar width after the described heat treatments shows that the α_2/γ-interface spacing deviates by not more than 30 nm between the alloys (Ti-44Al: 230 nm; Ti-44Al-5Nb: 230 nm; Ti-44Al-5Ta: 266 nm; Ti-44Al-5Zr: 237 nm).

3.2 Density of the alloys

In Table 2 the density of the investigated alloys is displayed. It is clear to see, that all three alloying elements increase the density in comparison to the binary alloy.

Table 2

Density in gcm^{-3} of the four investigated alloys, measured via Archimedes' principle.

Alloy	Ti-44Al	Ti-44Al-5Nb	Ti-44Al-5Ta	Ti-44Al-5Zr
Density [gcm^{-3}]	3.9103	4.1193	4.5530	4.0333

3.3 Segregation of alloying elements

All alloys show a typical cast microstructure after the arc melting process. During solidification through the two-phase field (β + liquidus), β-dendrites grow into the melt. At lower temperatures, the β-phase dendrites are surrounded by the solidifying α-phase. After the solution heat treatment at 1380°C in the single phase α-region and subsequent cooling, the fully lamellar microstructure forms, but the former dendritic structure can still be discerned from the EPMA maps in Figure 3 [38,39].

However, the segregation of the alloying elements Nb, Ta and Zr is less pronounced and a more homogeneous distribution is achieved after solution heat treatment, compared to the as-cast state of the alloys.

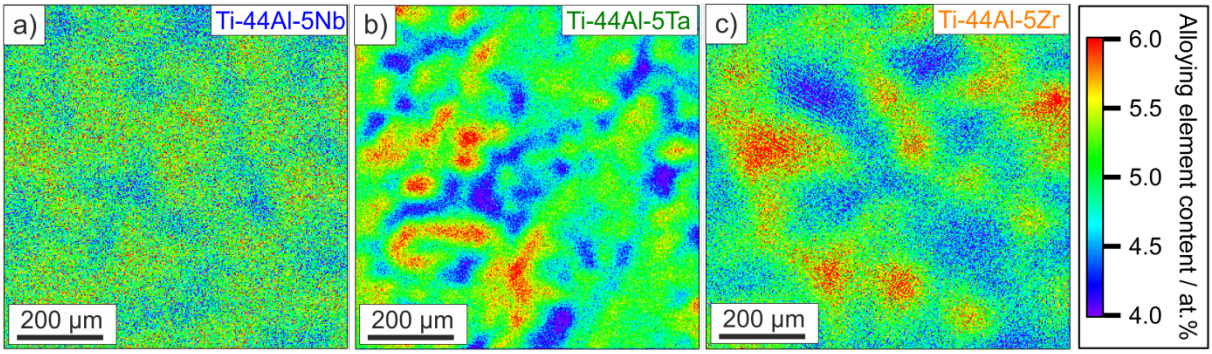

Figure 3 EPMA-maps of alloying elements X in Ti-44Al-5X alloys. a) X= Nb, b) X= Ta and c) X= Zr after a heat-treatment of 1380°C for 1h with a cooling rate of 5 $Kmin^{-1}$.

The EPMA-maps in Figure 3 show that the concentration of the elements Nb, Ta and Zr varies in a range of 4 at.% and 6 at.% between the dendrite cores and interdendritic regions after the solution heat treatment. Distinct differences in the distribution of the alloying elements are also visible. Ta and Zr show a much stronger segregation than Nb and the average distance between the dendrite cores is much smaller in the Ta-containing alloy compared to the Nb- and Zr-containing alloys. This is illustrated by the segregation coefficients and the dendrite core distances presented in Table 3.

Table 3

Segregation coefficient k* of the alloying elements Nb, Ta and Zr in the ternary alloys and the average spacing between concentration maxima and concentration minima (standard deviation is given in brackets)

Alloy	Segregation coefficient k*	Dendrite spacing /µm
Ti-44Al-5Nb	1.2972	226.79 (± 72.84)
Ti-44Al-5Ta	1.4702	149.12 (± 60.57)
Ti-44Al-5Zr	1.4441	231.56 (± 67.08)

The segregation coefficient, k^* of the alloying element was calculated using the EPMA results and equation 2, where $c_{interdendritic}$ corresponds to the concentration of the element in the

interdendritic area and $c_{dendritic}$ is the concentration of the alloying element in the dendrite core.

$$k^* = \frac{c_{dendritic}}{c_{interdendritic}} \quad (2)$$

3.4 Creep behaviour

In Figure 4 the creep behavior of the binary and ternary alloys at 100 MPa and 900°C are shown in a strain vs. time plot (a) and a strain rate vs. strain plot (b). The binary alloy has the lowest creep strength, i.e. highest strain rate, followed by the Nb-containing alloy. The creep rates of the Zr-containing and Ta-containing alloys are the lowest. The time to reach 5 % strain increases from 45.6 h to 84.7 h, 332.5 h or 482.5 h when adding 5 at%. of Nb, Zr or Ta to the binary Ti-44Al alloy. After the minimum creep rate is reached, all alloys show a slight increase of the creep rate in the secondary creep regime. This increase is related to microstructural changes during the creep exposure [40], which will be discussed in the following chapter 3.5.

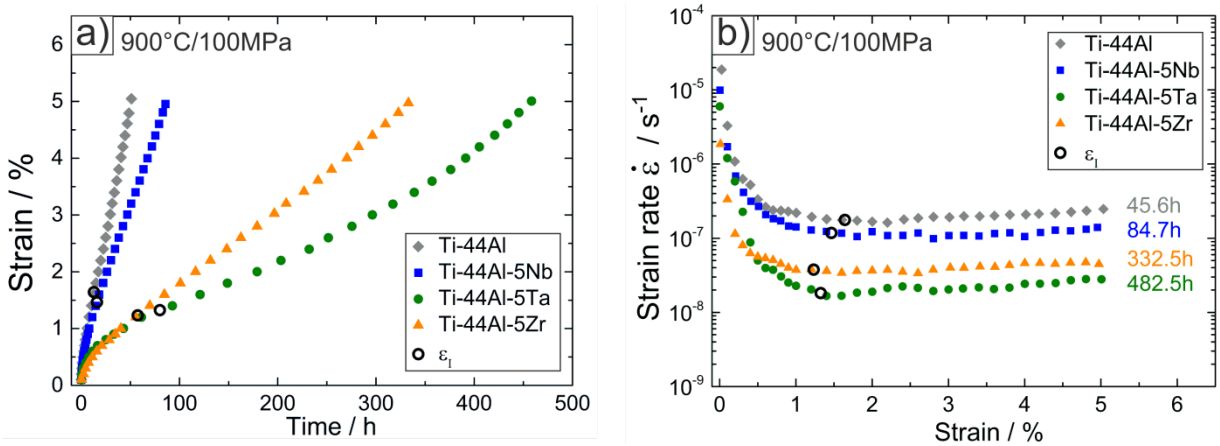

Figure 4 Creep curves of the four alloys at 900°C and 100 MPa load plotted a) strain over time and b) strain rate over strain. The lower strain rate results in a higher testing time until a plastic deformation of 5 % is reached. The end of the primary creep regime, ε_I, determined by the Garofalo-fit, is displayed in black, non-filled circles.

In Figure 5 the influence of the alloying elements on the creep properties is shown in a Norton-plat at 900°C. and stresses between 100 MPa and 250 MPa. The binary alloy has the lowest creep resistance at all stresses and all ternary alloys show a better creep behavior. Ti-44Al-5Nb has the lowest creep resistance of the ternary alloys, while Ti-44Al-5Ta and Ti-44Al-5Zr exhibit similar minimum creep rates which vary just a little.

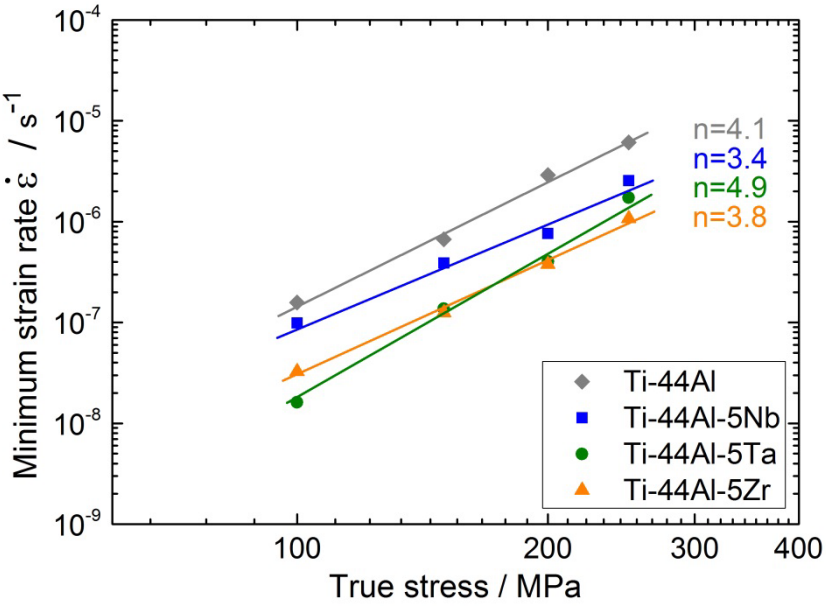

Figure 5 Norton-Plot of the performed creep tests. The stress exponent n was calculated from the slope of these curves.

The determined stress exponents n are in a range between 3.4 and 4.9, which indicates that the same deformation mechanisms of dislocation climb is active in all four alloys [41].

The end of the primary creep regime, ε_I, determined by fitting the creep curves using the Garofalo equation (equation 1) [27] is marked as black, non filled circles in Figure 4. A clear trend of the transition from the primary to the steady state creep regime as a function of stresses is not evident, however the average strain until the end of primary creep is reached, differs significantly between the alloys (see Figure 6). The results indicate that the alloying

elements influence the range of the primary creep regime in titanium aluminides, but not necessarily in the same way and order as they affect the minimum creep rate.

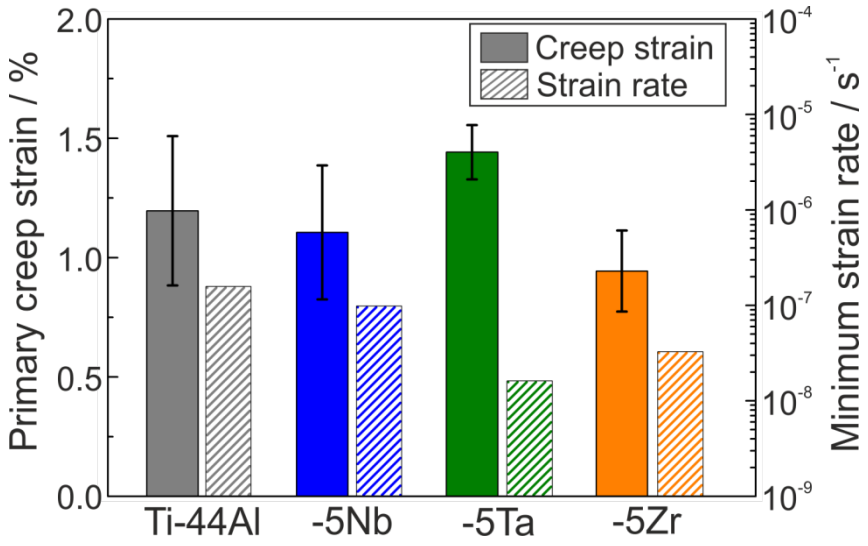

Figure 6 Average strain until the end of the primary creep regime is reached (left axis) and minimum strain rate (right axis) of all four alloys, tested at stresses at 900°C and 100 MPa.

Obviously, there is no clear difference between the binary Ti 44Al alloy and the Ti 44Al 5Nb alloy also considering the large standard deviation for determining the end of the primary creep regime. However, there are distinct differences between the Ta- and Zr-containing alloy.

In summary, it can be stated that all three alloying elements improve the creep resistance at 900°C and affect differently the end of the primary creep regime. Remarkably, the results demonstrate that both Ta and Zr lead to better creep properties compared to the alloying element Nb, which is one of the most common alloying elements in titanium aluminides and one of the main elements in the well-known alloys TNB and TNM [42,43].

3.5 Microstructural stability

In addition to the creep resistance, the microstructure of the crept samples was investigated to get a deeper understanding of the microstructure evolution during creep exposure and the influence of the alloying elements on the microstructural stability. In comparison to the microstructure before creep exposure the specimens show discontinuously coarsened areas (Figure 7a), the formation of γ-grains, a clearly deformed microstructure and a significant change in the lamellar width (Figure 7b) caused by a change in the γ-phase volume fraction.

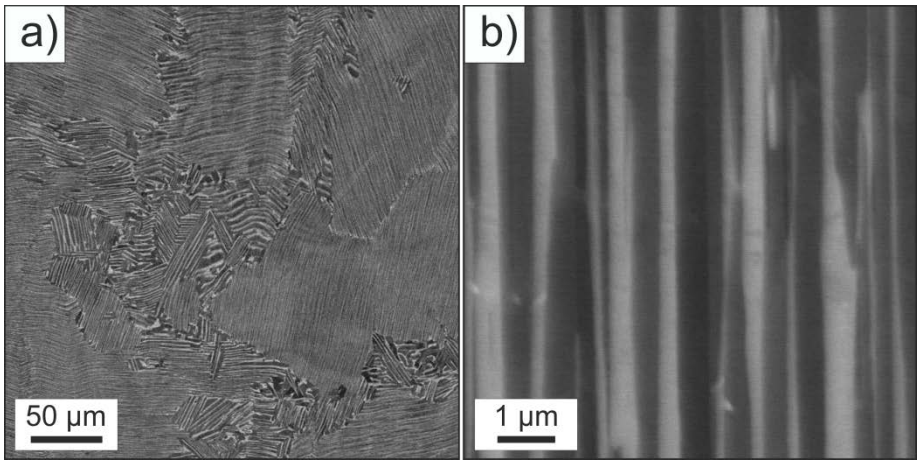

Figure 7 The microstructure of the binary Ti-44Al alloy after creep exposure at 900°C and 100 MPa load at different magnification shows a) discontinuous coarsened areas, and b) the dissolution of the $\boldsymbol{\alpha_2}$-phase after creep

The observed discontinuous coarsening is also reported in literature, where it has been observed in samples with relatively fine lamellar spacing [44–47] during creep experiments in the 900 - 1000°C range. In this work, all alloys show these discontinuously coarsened areas which still show a lamellar microstructure. Their formation is detrimental for the creep resistance and leads to an increase in the strain rate with increasing volume fraction [34]. This discontinuous coarsening process starts typically at the colony boundaries and grows further into the colony, thus it occurs through grain boundary diffusion [48,49]. The driving force of

this process is the reduction of the dislocation density as well as interface energy [44]. The creep tests are performed at 900°C, hence the heat-treated microstructure is not in an equilibrium state but probably has a too high α_2 volume fraction and the system wants to reach the phase equilibrium at the given temperature.

Several publications show a linear time dependence of the discontinuous coarsened area reaction in fully lamellar titanium aluminides [47,50]. On the other hand Qin et al. [48] described an extremely fast growth rate in the first hour of exposure and afterwards a relatively slow increase of the discontinuously coarsened area in binary alloys. In this work the coarsened areas of the Ti-44Al-5X alloys after 5 % plastic deformation and different testing times were investigated. Therefore it is reasonable to compare the areas normalized by the exposure time, because the discontinuous coarsening is a diffusion-assisted growth process of the lamellae [49,50].

The results in Figure 8 show that with increasing stress the coarsening rate increases, regardless which of the four investigated alloys is considered. This is in good accordance with the expectation, because a higher stress is associated with a higher dislocation density, which is a major driving factor for discontinuous coarsening. The comparison between the ternary alloys and the binary one reveals that all alloying elements, Nb, Ta and Zr, have a beneficial influence and reduce the discontinuous coarsening rate in fully lamellar titanium aluminides.

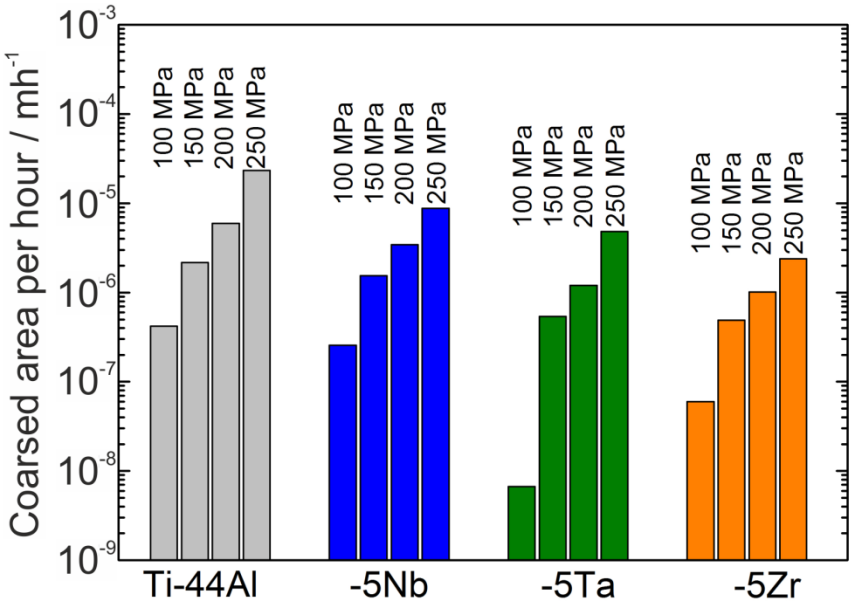

Figure 8 Discontinuously coarsened area per hour for the four investigated alloys at 900°C and different applied stresses.

Bartholomeusz and Wert [44] suggest that the rate controlling step in this coarsening process is a diffusion accommodated process of boundary movement. The coarsening process occurs via grain boundary migration, where the microstructure behind the moving boundary is significantly coarser then the initial lamellar microstructure. If this boundary movement is a diffusion controlled process, the diffusion rate of the alloying element is of major concern. If the diffusivity of the alloying element is slower than the self-diffusion of titanium, the boundary migration process should slow down through the addition of ternary elements and the discontinuous coarsening should be retarded, because all three elements occupy sites in the titanium-sublattice [51] in the two intermetallic phases. Another influencing factor could be the solubility in the two phases. If the solubility differs significantly, the growth of the coarser lamellae can be slowed down through redistribution of the alloying element in the coarser microstructure. According to Kainuma et al. [16] this is the case for Ta and Zr, because both partition unequally between the two phases. Consequently, the slower discontinuous coarsening in the ternary alloys could be caused by a combination of low

interdiffusion coefficients and unequal partitioning behavior in the case of Zr and Ta and by a lower interdiffusion coefficients in the case of Nb.

The second major microstructural change during the creep exposure is the growth of the γ-phase or respectively the degradation of the α_2-phase (Figure 7b). In comparison to the initial microstructure of the binary Ti-44Al the growth of the γ-phase is obvious (compare Figure 2b with Figure 7b). Before creep exposure, the alternating α_2- and γ-lamellae exhibit straight interfaces and lamellae of similar width over the whole colony. Afterwards the α_2-lamellae seem to be divided or interrupted by steps and ledges and the interface between the two phases is very rough in comparison to the pre-crept state. The dissolution of the α_2-phase and the subsequent growth of the γ-phase is well known in the literature [52–54]. Wang et al. [54] described the dissolution of the α_2-lamellae during creep with an fragmentation and spherodization process which can be caused by a subgrain boundary groove mechanism or an intersection of deformation twins with the α_2-lamellae.

To quantify the volume fraction of the two phases, the lamellar width of the α_2- and γ-phase before and after the creep tests is measured and the volume fraction of each phase is subsequently calculated. Because of the different testing times, the volume fraction is again normalized and a γ-phase growth rate of the different alloys at the tested stresses is plotted in Figure 9. The results show again the beneficial influence of the three alloying elements at all stresses in contrast to the unalloyed titanium aluminide. Larson et al. [20] found a similar α_2-phase stabilizing effect of W with respect to coarsening and dissolution. It was suggested that during creep exposure the alloying element segregates to the interface and decelerate the dissolution of the α_2-phase. If this is also assumed for the three investigated elements, it could explain the superior behavior of the ternary alloys in comparison to the binary alloy. However, in addition to reduced dissolution kinetics, an increased phase stability or a reduced

lattice misfit or a combination of these three could be also the reason for the α_2-stabilizing effect of Nb, Ta and Zr.

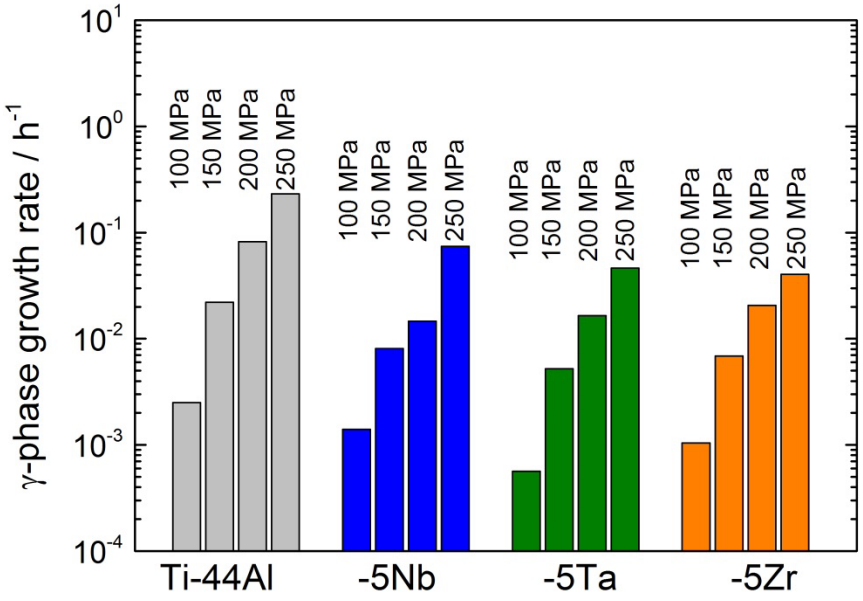

Figure 9 The γ-phase growth rate of the four alloys at different stresses. The beneficial influence of the alloying elements at all stress levels is clear to see.

4. Discussion

In order to explain the observed differences in creep strength, multiple factors such as solid solution hardening, diffusivity, elemental partitioning between α_2- and γ-phase, lattice misfit, microstructural stability, etc. have to be considered.

Due to the atomic size mismatch between the alloying element and the host Ti atom, the induced stress-fields interact with the dislocations. In Figure 10 the Goldschmidt radii of Ti compared to the three alloying elements are displayed, because all three alloying elements substitute Ti in the γ-phase and α_2-phase [51]. Nb and Ta are only slightly larger than Ti, while Zr is by far the largest atom, indicating a strong solid solution hardening effect of Zr by paraelastic interactions with dislocations.

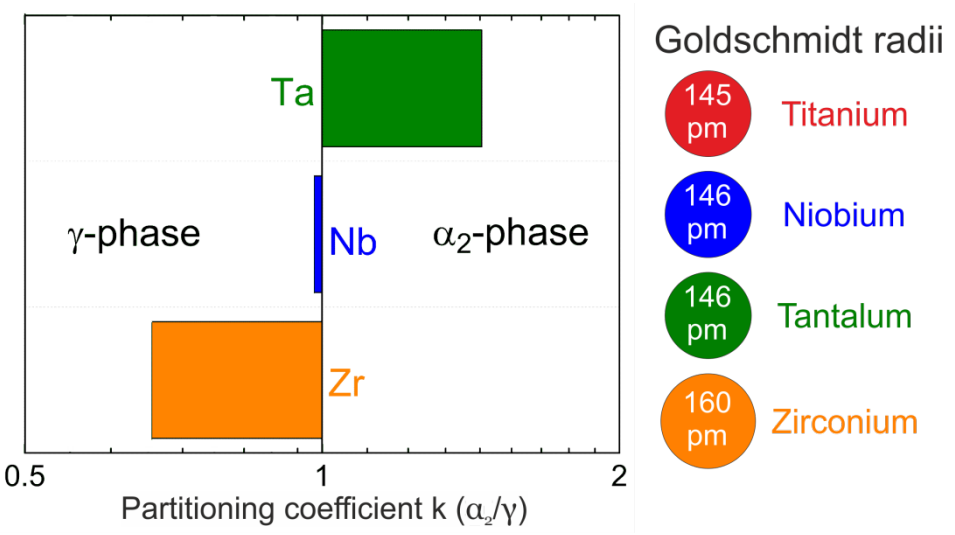

Figure 10 Partitioning coefficient of the three alloying elements and the Goldschmidt radii of the three alloying elements and Titanium.[16]

Another factor that should affect the creep properties is the diffusivity of the alloying element. Herzig et al. [55] investigated the diffusion behavior of several elements including Nb and Zr in the γ-phase, but for Ta no data has been found in the literature. It was found that Zr diffuses much faster than Nb and therefore it should be less beneficial for retarding diffusion-controlled processes, such as dislocation climb. However, not only the solid solution hardening effect or the diffusivity of the alloying element play an important role, also the concentration of the alloying element in the γ-phase is crucial. The higher the concentration of the alloying element in the γ-phase, which deforms primarily during deformation due to lower strength [56–58], the stronger the total solid solution hardening effect or the influence on diffusion controlled processes of the alloying element. In Figure 10 the α_2/γ partitioning coefficients according to Kainiuma et al. [16] are shown. Ta mainly enriches in the α_2-phase, Nb partitions more or less equally between both phases and Zr is enriched mainly in the γ-phase. Accordingly, the high solubility of Zr in the γ-phase combined with the strong solid solution hardening effect could be the main reason for the excellent creep properties of the Zr-containing alloy. On the other side, the excellent properties of the Ta-containing alloy can

only be explained by an interdiffusion coefficient of Ta that is the lowest among the three investigated elements.

The different atomic size and partitioning behavior also means that the average lattice parameter of the two phases and therefore the α_2/γ lattice misfit changes through the addition of the ternary elements. Combining the partitioning coefficient of Kainuma et al. [16] with the calculations of Koizumi et al. [25] on the influence of alloying elements on the lattice parameter, the variation on the lattice misfit can be estimated theoretically for the three ternary alloys. Nb and Ta should increase the α_2/γ-lattice misfit, whereas Zr should decrease it. The lower the lattice misfit and coherency stresses at the same externally applied stresses, the lower the dislocation emission at the interface [8]. Accordingly, smaller coherency stresses should lead to a shorter primary creep regime, because lower strains are necessary until the equilibrium of dislocation emission and thermally activated dislocation annihilation is reached. This assumption correlates well with the observed effect of the alloying elements on the range of the primary creep regime and can explain the shorter primary creep regime of the Zr-containing alloy and the longer one of the Ta-containing alloy.

5. Summary and conclusion

A systematic study was performed to determine the influence of the three alloying elements Nb, Ta and Zr on the microstructure and creep properties of fully lamellar titanium aluminides. The following conclusions can be drawn:

- 5 at.% of the alloying elements Nb, Ta and Zr significantly increase the creep resistance.
- Nb leads to a smaller improvement in the creep properties in comparison to the addition of Ta and Zr.

- The addition of Zr shortens the primary creep regime, whereas Ta prolongs it.
- Nb, Ta and Zr decrease the average α_2/γ interface spacing, in comparison to the binary alloy.
- Nb, Ta and Zr improve the microstructural stability during creep exposure by slowing down the discontinuous coarsening and the transformation of the α_2-phase to the γ-phase.

Acknowledgment

The work was supported by the German Science Foundation (DFG) within the framework of DFG graduate school 1229. The authors would like to acknowledge Dipl.-Geol. Sabine Michel for the EPMA measurements, B. Sc. Bastian Zettl for the support in the microstructural analysis and Dr. Jonathan D. H. Paul and M. Sc. M. Rackel for processing the four different alloys.

Literature

[1] Y.-W. Kim, Intermetallic alloys based on gamma titanium aluminide, JOM J. Miner. Met. Mater. Soc. 41 (1989) 24–30.

[2] T. Tetsui, S. Ono, Endurance and composition and microstructure effects on endurance of TiAl used in turbochargers, Intermetallics. (1999) 689–697.

[3] P. Janschek, Wrought TiAl Blades, Mater. Today Proc. 2, Supplement 1 (2015) S92–S97. doi:http://dx.doi.org/10.1016/j.matpr.2015.05.024.

[4] B.D. Worth, J.W. Jones, J.E. Allison, Creep deformation in near-γ TiAl: I. the influence of microstructure on creep deformation in Ti-49Al-1V, Metall. Mater. Trans. A. 26 (1995) 2947–2959. doi:10.1007/BF02669651.

[5] M.J. Blackburn, Some aspects of phase transformation in titanium alloys, in: R.I. Jaffee, N.E. Promisel (Eds.), Sci. Technol. Appl. Titan., Pergamon, 1970: pp. 633–643.

[6] P.M. Hazzledine, Coherency and loss of coherency in lamellar TiAl, Intermetallics. (1998) 673–677.

[7] F. Appel, U. Brossmann, U. Christoph, S. Eggert, P. Janschek, U. Lorenz, J. Müllauer, M. Oehring, J.D.H. Paul, Recent Progress in the Development of Gamma Titanium Aluminide Alloys, Adv. Eng. Mater. 2 (2000) 699–720.

[8] F. Appel, U. Christoph, M. Oehring, Creep deformation in two-phase titanium aluminide alloys, Mater. Sci. Eng. A. 329–331 (2002) 780–787. doi:10.1016/S0921-5093(01)01633-1.

[9] C. Wen, K. Yasue, J. Lin, Y. Zhang, C. Chen, The effect of lamellar spacing on the creep behavior of a fully lamellar TiAl alloy, Intermetallics. 8 (2000) 525–529.

[10] M. Yamaguchi, H. Zhu, M. Suzuki, K. Maruyama, F. Appel, Importance of microstructural stability in creep resistance of lamellar TiAl alloys, Mater. Sci. Eng. A. 483–484 (2008) 517–520. doi:10.1016/j.msea.2006.09.147.

[11] B.D. Worth, J.W. Jones, J.E. Allison, Creep deformation in near-γ TiAl: II. influence of carbon on creep deformation in Ti-48Al-1V-0.3C, Metall. Mater. Trans. A. 26 (1995) 2961–2972. doi:10.1007/BF02669652.

[12] E. Hamzah, M. Kanniah, M. Harun, Effect of chromium addition on microstructure and creep strength of as-cast Ti–48Al alloy, Mater. Sci. Eng. A. 483–484 (2008) 555–559. doi:10.1016/j.msea.2006.11.168.

[13] W.J. Zhang, G.L. Chen, F. Appel, T.G. Nieh, S.C. Deevi, A preliminary study on the creep behaviour of Ti-45Al-10Nb alloy, Mater. Sci. Eng. A. (2001) 250–253.

[14] J. Lapin, T. Pelachová, M. Dománková, Creep behaviour of a new air-hardenable intermetallic Ti–46Al–8Ta alloy, Intermetallics. 19 (2011) 814–819. doi:10.1016/j.intermet.2010.11.023.

[15] D. Vojtěch, T. Popela, J. Hamáček, J. Kützendörfer, The influence of tantalum on the high temperature characteristics of lamellar gamma+alpha 2 titanium aluminide, Mater. Sci. Eng. A. 528 (2011) 8557–8564. doi:10.1016/j.msea.2011.07.070.

[16] R. Kainuma, Y. Fujita, H. Mitsui, I. Ohnuma, K. Ishida, Phase equilibria among alpha (hcp), beta (bcc) and gamma (L10) phases in TiAl base ternary alloys, Intermetallics. (2000) 855–867.

[17] S. Divinski, F. Hisker, C. Klinkenberg, C. Herzig, Niobium and titanium diffusion in the high niobium-containing Ti–54Al–10Nb alloy, Intermetallics. 14 (2006) 792–799. doi:doi:10.1016/j.intermet.2005.12.007.

[18] J.P. Lin, X.J. Xu, Y.L. Wang, S.F. He, Y. Zhang, X.P. Song, G.L. Chen, High temperature deformation behaviors of a high Nb containing TiAl alloy, Intermetallics. 15 (2007) 668–674. doi:10.1016/j.intermet.2006.10.029.

[19] Z.C. Liu, J.P. Lin, S.J. Li, G.L. Chen, Effects of Nb and Al on the microstructures and mechanical properties of high Nb containing TiAl base alloys, Intermetallics. 10 (2002) 653–659.

[20] D.J. Larson, C.T. Liu, M.K. Miller, Microstructural characterization of segregation and precipitation in α2+γ titanium aluminides, Mater. Sci. Eng. A. 239–240 (1997) 220–228. doi:https://doi.org/10.1016/S0921-5093(97)00585-6.

[21] M.H. Loretto, Z. Wu, M.Q. Chu, H. Saage, D. Hu, M.M. Attallah, Deformation of microstructurally refined cast Ti46Al8Nb and Ti46Al8Ta, Intermetallics. 23 (2012) 1–11. doi:10.1016/j.intermet.2011.12.012.

[22] T.T. Cheng, M.R. Willis, Effects of aging on the microstructure and creep properties of γ-TiAl containing heavy alloying, Scr. Mater. 39 (1998) 1255–1265.

[23] T. Kawabata, H. Fukai, O. Izumi, Effect of ternary additions on mechanical properties of TiAl, Acta Mater. 46 (1998) 2185–2194.

[24] T. Cheng, M. Willis, I. Jones, Effects of major alloying additions on the microstructure and mechanical properties of γ-TiAl, Intermetallics. 7 (1999) 89–99.

[25] Y. Koizumi, M. Yoshiya, A. Sugihara, Y. Minamino, Effect of impurity atoms on α_2/γ lamellar interfacial misfit in Ti–Al alloy: a systematic first principles study, Philos. Mag. 91 (2011) 3685–3704. doi:10.1080/14786435.2011.588971.

[26] X.-W. Du, J. Wang, J. Zhu, Segregation of alloying elements in a fully lamellar TiAl alloy, Scr. Mater. 45 (2001) 19–24.

[27] D. Dieter E., Mechanical Metallurgy, McGraw-Hill Book Company, New York, 1961.

[28] F. Appel, P.A. Beaven, R. Wagner, Deformation processes related to interfacial boundaries in two-phase γ-titanium aluminides, Acta Metall. Mater. 41 (1993) 1721–1732. doi:https://doi.org/10.1016/0956-7151(93)90191-T.

[29] F. Appel, R. Wagner, Microstructure and deformation of two-phase y-titanium aluminides, Mater. Sci. Eng. R. 22 (1998) 187–268.

[30] Y.-W. Kim, D.M. Dimiduk, Progress in the understanding of gamma titanium aluminides, JOM. 43 (1991) 40–47. doi:10.1007/BF03221103.

[31] J. Triantafillou, J. Beddoes, L. Zhao, W. Wallace, Creep properties of near γ-TiAl+W with a lamellar microstructure, Scr. Metall. Mater. 31 (1994) 1387–1392. doi:http://dx.doi.org/10.1016/0956-716X(94)90123-6.

[32] K. Maruyama, M. Yamaguchi, G. Suzuki, H. Zhu, H.Y. Kim, M.H. Yoo, Effects of lamellar boundary structural change on lamellar size hardening in TiAl alloy, Acta Mater. 52 (2004) 5185–5194. doi:10.1016/j.actamat.2004.07.029.

[33] M. Charpentier, A. Hazotte, D. Daloz, Lamellar transformation in near-γ TiAl alloys—Quantitative analysis of kinetics and microstructure, Mater. Sci. Eng. A. 491 (2008) 321–330. doi:10.1016/j.msea.2008.02.009.

[34] S. Zghal, M. Thomas, S. Naka, A. Finel, A. Couret, Phase transformations in TiAl based alloys, Acta Mater. 53 (2005) 2653–2664. doi:https://doi.org/10.1016/j.actamat.2005.02.025.

[35] S. Zghal, M. Thomas, A. Couret, Structural transformations activated during the formation of the lamellar microstructure of TiAl alloys, Intermetallics. 13 (2005) 1008–1013. doi:https://doi.org/10.1016/j.intermet.2004.12.009.

[36] F. Appel, M. Oehring, J.D.H. Paul, eds., Gamma Titanium Aluminide Alloys - Science and Technology, Wiley-VCH, Weinheim, 2009.

[37] X. Wu, Review of alloy and process development of TiAl alloys, Intermetallics. 14 (2006) 1114–1122. doi:http://dx.doi.org/10.1016/j.intermet.2005.10.019.

[38] C. McCullough, J.J. Valencia, C.G. Levi, R. Mehrabian, Phase equilibria and solidification in Ti-Al alloys, Acta Metall. 37 (1989) 1321–1336. doi:http://dx.doi.org/10.1016/0001-6160(89)90162-4.

[39] V.T. Witusiewicz, A.A. Bondar, U. Hecht, J. Zollinger, L.V. Artyukh, T.Y. Velikanova, The Al–B–Nb–Ti system, J. Alloys Compd. 474 (2009) 86–104. doi:10.1016/j.jallcom.2008.06.128.

[40] S. Bystrzanowski, A. Bartels, H. Clemens, R. Gerling, F.P. Schimansky, G. Dehm, H. Kestler, Creep behaviour and related high temperature microstructural stability of Ti–46Al–9Nb sheet material, Intermetallics. 13 (2005) 515–524. doi:http://dx.doi.org/10.1016/j.intermet.2004.09.001.

[41] M.E. Kassner, M.-T. Pérez-Prado, Fundamentals of creep in metals and alloys, Elsevier, Amsterdam, 2004.

[42] M. Naveed, A.F. Renteria, S. Weiß, Role of alloying elements during thermocyclic oxidation of β/γ-TiAl alloys at high temperatures, J. Alloys Compd. 691 (2017) 489–497. doi:10.1016/j.jallcom.2016.08.259.

[43] E. Schwaighofer, B. Rashkova, H. Clemens, A. Stark, S. Mayer, Effect of carbon addition on solidification behavior, phase evolution and creep properties of an

intermetallic b-stabilized g-TiAl based alloy, Intermetallics. 46 (2014) 173–184. doi:http://dx.doi.org/10.1016/j.intermet.2013.11.011.

[44] M.F. Bartholomeusz, J.A. Wert, The effect of thermal exposure on microstructural stability and creep resistance of a two-phase TiAl/Ti3Al lamellar alloy, Metall. Mater. Trans. A. 25 (1994) 2371–2381.

[45] P. Pouly, M.-J. Hua, C.I. Garcia, A.J. DeArdo, Isothermal transformation behavior of near-gamma TiAl alloys, Scr. Metall. Mater. 29 (1993) 1529–1534. doi:http://dx.doi.org/10.1016/0956-716X(93)90272-T.

[46] M. Beschliesser, A. Chatterjee, A. Lorich, W. Knabl, H. Kestler, G. Dehm, H. Clemens, Designed fully lamellar microstructures in a γ-TiAl based alloy: adjustment and microstructural changes upon long-term isothermal exposure at 700 and 800°C, Mater. Sci. Eng. A. 329 (2002) 124–129. doi:http://dx.doi.org/10.1016/S0921-5093(01)01545-3.

[47] D.S. Shong, Y.-W. Kim, Discontinuous coarsening of high perfection lamellae in titanium aluminides, Scr. Metall. 23 (1989) 257–261. doi:http://dx.doi.org/10.1016/0036-9748(89)90422-5.

[48] G. Qin, J. Wang, S. Hao, Discontinuous coarsening of primary α 2/γ lamellae at colony boundaries in γ-TiAl-based alloys, Intermetallics. 7 (1999) 1–4.

[49] A. Denquin, S. Naka, Phase transformation mechanisms involved in two-phase TiAl-based alloys—I. Lambellar structure formation, Acta Mater. 44 (1996) 343–352.

[50] J.Y. Jung, J.K. Park, Growth kinetics of discontinuous coarsening of lamellar structure in Ti–44at.% Al (–0.5 at.% Cr) intermetallic compounds, Acta Mater. 46 (1998) 4123–4130.

[51] Y.L. Hao, D.S. Xu, Y.Y. Cui, R. Yang, D. Li, The site occupancies of alloying elements in TiAl and Ti3Al alloys, Acta Mater. 47 (1999) 1129–1139. doi:http://dx.doi.org/10.1016/S1359-6454(99)00006-3.

[52] W.F. Cui, C.M. Liu, Fracture characteristics of γ-TiAl alloy with high Nb content under cyclic loading, J. Alloys Compd. 477 (2009) 596–601. doi:http://dx.doi.org/10.1016/j.jallcom.2008.10.118.

[53] D. Hu, A.B. Godfrey, M.H. Loretto, Thermal stability of a fully lamellar Ti-48Al-2Cr-2Nb-1B alloy, Intermetallics. 6 (1998) 413–417. doi:http://dx.doi.org/10.1016/S0966-9795(98)80019-8.

[54] J.G. Wang, L.M. Hsiung, T.G. Nieh, Microstructural instability in a crept fully lamellar TiAl alloy, Intermetallics. 7 (1999) 757–763. doi:http://dx.doi.org/10.1016/S0966-9795(98)00125-3.

[55] C. Herzig, T. Przeorski, M. Friesel, F. Hisker, S. Divinski, Tracer solute diffusion of Nb, Zr, Cr, Fe, and Ni in γ-TiAl: effect of preferential site occupation, Intermetallics. 9 (2001) 461–472.

[56] M. Es-Souni, Effects of microstructure and alloy composition on strength and creep properties of gamma TiAl base alloys, in: High Perform. Mater. Engine Technol. Proc. Top. Symp. V High Perform. Mater. Engine Technol. 8th CIMTEC-World Ceram. Congr. Forum New Mater. Florence Italy June 28 July 4 1994, Techna Group, 1995: p. 373.

[57] S. Gebhard, F. Pyczak, M. Göken, Microstructural and micromechanical characterisation of TiAl alloys using atomic force microscopy and nanoindentation, Mater. Sci. Eng. A. 523 (2009) 235–241. doi:10.1016/j.msea.2009.05.068.

[58] F. Iqbal, F. Pyczak, S. Neumeier, M. Göken, Crack nucleation and elastic / plastic deformation of TiAl alloys investigated by in-situ loaded atomic force microscopy, Mater. Sci. Eng. A. 689 (2017) 11–16. doi:10.1016/j.msea.2017.02.017.